www.ietdl.org

Published in IET Generation, Transmission & Distribution
Received on 11th August 2013
Revised on 6th December 2013
Accepted on 17th December 2013
doi: 10.1049/iet-gtd.2013.0562

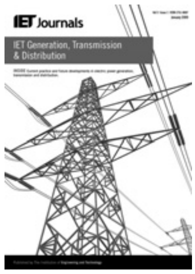

ISSN 1751-8687

Artificial neural network model of photovoltaic generator for power flow analysis in PSS®SINCAL

Travis Xu[1], *Bala Venkatesh*[1], *Chandrabhanu Opathella*[1], *Birendra N. Singh*[2]

[1]*Centre for Urban Energy, Ryerson University, Toronto, Canada*
[2]*Hydro One Networks Inc., Toronto, Canada*
E-mail: bala@ryerson.ca

Abstract: Output of a three-phase photovoltaic generator (PVG) is a function of sunlight irradiance, temperature, and three-phase terminal voltage phasors. Three-phase PVGs are largely connected to rural distribution systems feeders that are predominantly unbalanced. Models of PVGs that are only a function of sunlight irradiance and temperature disregarding unbalanced three-phase terminal voltages phasors are simple to use with three-phase power flow analysis but yield inaccurate solutions. Detailed three-phase PVG models are complex and non-linear, hence unsuitable for power flow analysis applications. This study proposes an artificial neural network (ANN) model to represent a PVG comprising photovoltaic panels, a boost chopper and a three-phase inverter. Main advantages of the ANN model are that it can be readily used to model a PVG of any size and type, mathematical simplicity, high accuracy with unbalanced systems and computational speed. The model was tested with the unbalanced distribution system feeder from a Canadian utility. The results show that the ANN model of a PVG is computationally fast and more accurate than simple model that ignores unbalanced three-phase terminal voltage phasors. In addition, simplicity of the proposed ANN model of PVG allows easy integration into commercial software packages such as PSS®SINCAL as reported in this study.

1 Introduction

Photovoltaic generator (PVG) is one of the most rapidly developing renewable sources after wind energy [1]. Ontario (Canada) has a PVG capacity of about 500 MW online and has more than 1600 MW of additional PVG capacity contracted by June of 2012 [2]. Like other types of distributed generations, PVGs are normally connected to distribution systems (DSs) instead of transmission systems [3].

DSs are unbalanced because of the following reasons: (a) a large number of unevenly distributed single-phase loads, and, (b) conductor spacing of three-phase line segments are asymmetrical and they are seldom transposed [4]. DS automation needs fast, efficient and accurate power flow solutions that requires fast, efficient and accurate component model of PVGs. Therefore DS power flow studies considering single phase equivalent assuming balanced conditions yields inaccurate solutions. The state of a DS can be accurately determined only by solving complex bus power balance equations considering unbalanced three-phase system [5] and accurate models of PVGs. A variety of three-phase power flow analysis algorithms have been developed for analysing unbalanced distribution systems such as Newton–Raphson technique developed considering three-wire/four-wire distribution systems [5–21], power flow studies with rooftop PV panels [20] and ladder iterative technique [6].

Simple PQ models of PVGs as a function of solar irradiance and cell temperature but assuming nominal and balanced PCC (point of common coupling) voltage have been proposed in the past [8–10]. These models lead to erroneous DS Power Flow Solutions in an unbalanced DS because actual power output PVG is not equal among three phases. Details about the unbalanced power outputs are given in Section 2. An accurate three-phase model of PVGs is a function of three-phase terminal voltage phasors, solar irradiance and cell temperature and comprises a set of non-linear equations. Given above, PVG models that consider PCC three-phase voltage phasors and unequal power outputs are not available in publicly reported literature [5–21].

Power flow analysis algorithm solves bus-wise power balance equations and it is iterative as shown in Fig. 1. In each iterative step, PVG generation is recomputed using the most recent estimate of voltage solution. With several PVGs in a single DS, a complex model for PVG will significantly slow down any power flow algorithm. To overcome the challenge of higher computational effort, accuracy and difficulty to incorporate PVG models readily into commercial software, the use of artificial neural network (ANN) to model PVG is proposed in this paper. The use of ANN in PVG modelling is not new and in most cases ANN is used for solar irradiance forecasting [14], sizing of stand-alone PVG [15, 16], performance prediction [17], MPPT algorithms [19] etc.

An ANN model of a three-phase PVG with inverter is proposed in this paper that can be used for fast and accurate power flow analysis. The proposed ANN model for three-phase PVG is the function of irradiation, temperature, and three-phase PCC voltage phasors. The ANN model of PVG developed in this paper is independent of the power flow analysis technique or network topology. Unlike other

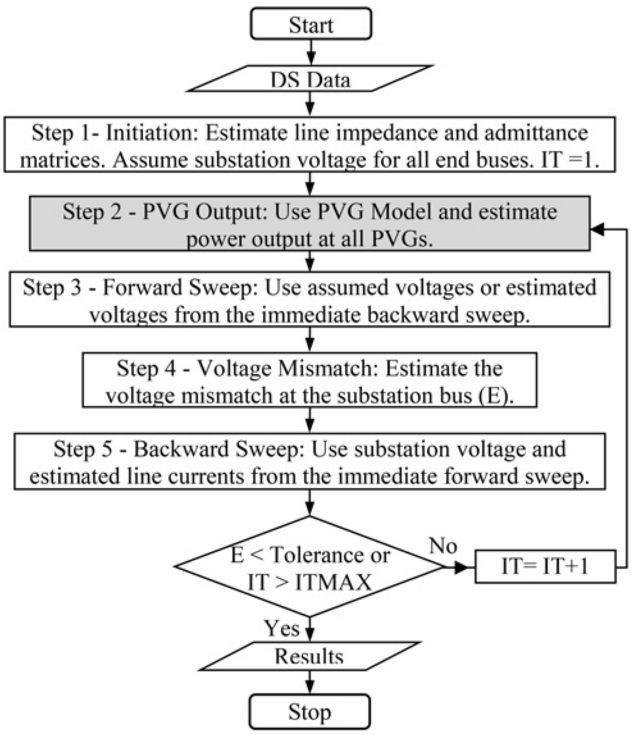

Fig. 1 *Block diagram showing the Ladder Iterative Technique power flow algorithm with PVG model [7]*

models, building an ANN model for three-phase PVG does not need to analyse the equivalent circuits or transfer functions of PVG. Instead, ANN models develop an empirical mapping of the input–output relationship using a given input–output data (pattern) set. If the data set is from measurements on the PVG, an accurate ANN model of this PVG can be developed as long as the measured date set covers input/output domain space. The process of generating patterns and building ANN model of PVGs are explained in detail in the following sections of this paper. The proposed ANN models can be extended to model solar farms of any area and capacity, which means that the ANN approach provides a universal PVG modelling technique for any type or size. In addition, as shall be seen later, the proposed ANN PVG model can be easily implemented in commercial software such as PSS®SINCAL.

Steps of this research work can be summarised as follows:

(a) PVG model is built in Matlab/Simulink platform that relates input and output vector domains.
(b) For various values of input vector, PVG model built in Matlab/Simulink platform is used to generate corresponding output vectors.
(c) This input–output training data set is used to train the ANN model of PVG. This training is completed in Matlab and it yields relational matrices of ANN model.
(d) These relational matrices of ANN model of PVG are incorporated into PSS®SINCAL. This allows the use of accurate ANN models of PVG for power flow analysis without a significant impact on execution time.

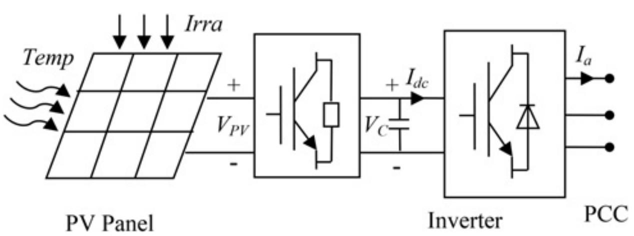

Fig. 2 *Common structure of PVG interface*

2 Accurate model of PVGs and effect of three-phase voltage imbalance

PVGs are always companied with single-phase or three-phase inverters. For the single-phase inverter, all the power generated by the PVG is injected through the inverter to one phase [20, 21]. However, when a PVG is connected through a three-phase inverter, power outputs in the three phases are equal only when the terminal voltages are balanced. PCC voltages in DS are seldom balanced and hence power outputs through three phases are unequal. With three-phase PVGs on a DS feeder, the problem of imbalance is compounded. DS power flow solutions with PVG models that ignore PCC voltage phasors tend to be erroneous.

To further explore effects of PCC voltage imbalance, a common structure of PVG interface is studied as shown in Fig. 2 where Irra and Temp are solar irradiance and ambient temperature, respectively. The purpose of the DC–DC converter is to boost the output voltage of PV panel. Normally a maximum power point track (MPPT) technique is used control the DC–DC converter to achieve the maximum output power from PV panel in all situations. The MPPT technique is implemented in DC–DC converter by adjusting $V_{\rm PV}$ against the current of PV panel [11, 12].

In most cases, voltage source inverters are used in PVG implementation and the pulse-width modulation (PWM) technique is used for inverter control. The inverter control objectives include keeping V_C constant and unity power factor control. The block diagram of the inverter control system is shown in Fig. 3, in which C is the capacitor between inverter and DC–DC converter, and $\varphi_{\rm V\_PCC}$ is the phase angle of PCC voltage. The proportional–integral controller is commonly used in PWM control. The variables with superscript ‘*’ indicate the command of controller. The unity power factor control is achieved by forcing $I_{\rm ac}$

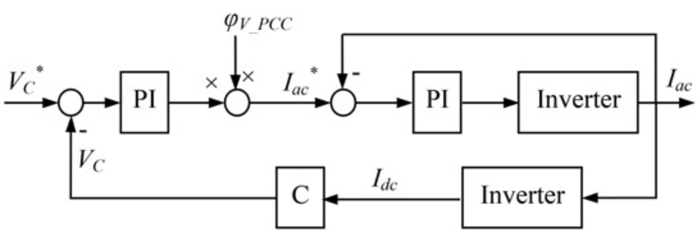

Fig. 3 *Block diagram of inverter control system*

having the same phase angle with V_{pcc}, assuming that three phases are balanced.

The model was implemented in Matlab/Simulink environment. Details of the controller are provided in the [13]. An example of the extent of imbalance in phase power with voltage magnitude and angle imbalance is shown in Table 1 considering a 1 MW PVG connected to a three-phase 600 V distribution system. The data comes from Matlab/Simulink simulation in which power base and voltage base are set to 1/3 MVA and 600 V, respectively. The solar irradiance and temperature are fixed at 1000 w/m^{-2} and 0°C during the two simulations.

The total real power flowing out of the panel is same in the two cases and the difference between the total powers reaching PCC arises due to different losses within PVG. If the three-phase voltage at PCC is balanced, the per phase power outputs are equal and equal to the one-thirds of maximum power that PVG could produces from the sunlight. However, if the PCC voltage is unbalanced, the per phase power outputs are unequal.

Reviewing the balanced case in Table 1, the difference between three-phase powers in Case 2 is 6.7% while the phase powers are equal to one-thirds of PVG power in the balanced Case 1. It is obvious that representing PVGs using balanced *PQ* values as a function of sunlight irradiation and temperature without accounting voltage unbalances at the point of connection with DS is inaccurate.

2.1 Model of PVG

According to the above analysis, the output active and reactive power of each phase is affected by the solar irradiance, temperature and voltage phasors of each phase as shown in Fig. 4, which can be written as follows

$$\left(P_a, Q_a, P_b, Q_b, P_c, Q_c\right) = f\left(\text{Irra}, \text{Temp}, V_a, \varphi_c, V_b, \varphi_b, V_c, \varphi_c\right) \tag{1}$$

where P_a, Q_a, P_b, Q_b, P_c and Q_c are the output active power and reactive power of three phases, respectively. Irra is the solar irradiance. Temp is the cell temperature. V_a, φ_a, V_b, φ_b, V_c and φ_c are the voltage magnitude and phase angle of three phases, respectively.

The simulation model for PVG with a three-phase inverter can be built in MATLAB/SIMULINK environment, but it is

Table 1 Power output variations for different PCC voltages (results from Matlab Simulink)

	Phase *a*	Phase *b*	Phase *c*
Case 1: balanced PCC voltage			
phase voltage at PCC	0.94∠0° pu	0.94∠−120° pu	0.94∠120° pu
phase active powers	0.9851 pu	0.9812 pu	0.9835 pu
total active power		2.9498 pu	
phase reactive powers	0.0013 pu	0.0009 pu	−0.0023 pu
case 2: unbalanced PCC voltage			
phase voltage at PCC	0.99∠3° pu	1.06∠−122° pu	0.94∠115° pu
phase real powers	0.9480 pu	1.0120 pu	0.9966 pu
total real power		2.9566 pu	
phase reactive powers	0.1335 pu	−0.0731 pu	−0.0701 pu

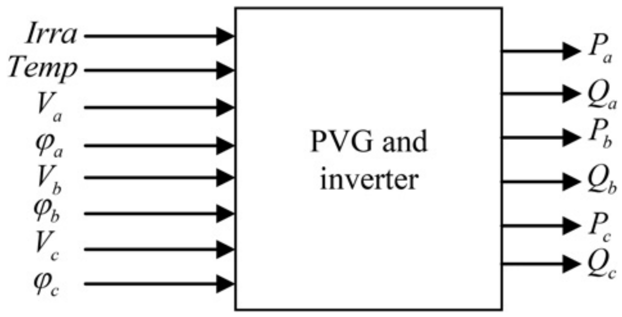

Fig. 4 *Factors affecting output power of PVG*

time consuming to run. It is difficult, if not impossible, to use this MATLAB/SIMULINK model for power flow analysis, not to mention their incorporation into a commercial software.

3 Ann model of PVG

3.1 ANN technique

An ANN maps an input space to an output space, and the mapping is built by training the ANN using input–output data pairs [18]. Once the ANN is well trained, the desired output can be gotten for an input using the mapping relationship possessed within the ANN.

A typical feed-forward ANN is used to model PVGs in this paper. The typical architecture of the feed-forward neural network is shown in Fig. 5. In this paper, l is the notation for the lth hidden layer of an ANN whereas 0 for the input layer and L for the output layer. The variable x is the input for ANN and the variable y is the output of ANN. The number of neurons in input layer N_0 and the number of neurons in output layer N_L are determined by (1). The number of hidden layers $L-1$ and the number of neurons in the lth hidden layer N_l is prudently chosen such that training time is the least and the mapping is most accurate.

A neuron in hidden layer or output layer is formed by one or more inputs, a functional element and an output. Fig. 6 shows the structure of the jth neuron in the lth layer. In Fig. 6, o_j^l is the output of the jth neuron in the lth layer. The variable w_{ji}^l is the weight of connection between the ith neuron in the $(l-1)$th layer and the jth neuron in the lth layer. The variable ω_j^l is the bias of the jth neuron in the lth layer which is usually considered as a weight of connection between a neuron with constant output 1 and this neuron.

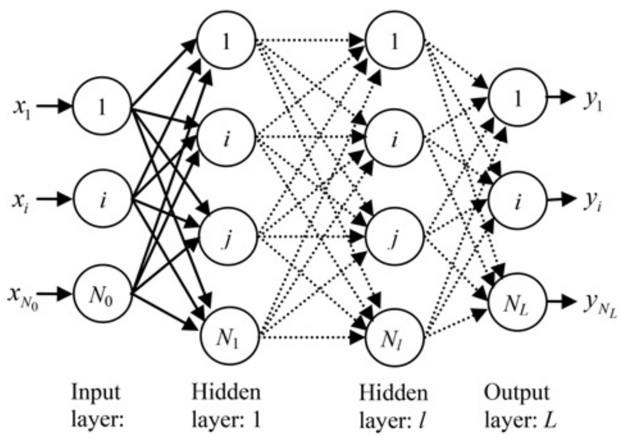

Fig. 5 *Multiplayer feed-forward neural network*

IET Gener. Transm. Distrib., 2014, Vol. 8, Iss. 7, pp. 1346–1353
doi: 10.1049/iet-gtd.2013.0562

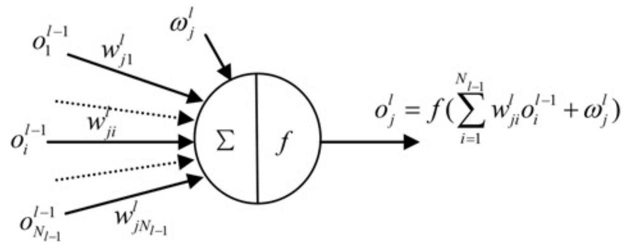

Fig. 6 *Neuron in hidden layer or output layer*

The neurons in input layer have only one input and no functional element.

In each iterative training step, the error at the output layer back propagates to each hidden layer to adjust the weights. The weight update equation is as [18]

$$\Delta w_{ji}^l = -\eta \frac{\partial E}{\partial o_j^l} o_i^{l-1} \dot{f} \left(\sum_{i=1}^{N_{l-1}} w_{ji}^l o_i^{l-1} + \omega_j^l \right) \tag{2}$$

where η is the learning rate and E is the output error which can be written as

$$E = \frac{1}{2} \sum_{i=1}^{N_L} (t_i - y_i)^2 \tag{3}$$

where t_i is the target value of the ith output neuron in a certain training pattern. The partial differential in (2) can be written as

$$\frac{\partial E}{\partial o_j^l} = \sum_{i=1}^{N_{l+1}} \frac{\partial E}{\partial o_i^{l+1}} \frac{\partial o_i^{l+1}}{\partial o_j^l}, \quad 0 < l < L \tag{4}$$

ANN model training algorithm was programmed in Matlab. At the first iterative step, random weights and bias were assigned. Then the output of every node in each layer was calculated by feed-forwarding the inputs of ANN (outputs of nodes in the input layer). When the outputs of ANN (outputs of nodes in the output layer) were obtained, error between outputs and targets was calculated using (3). Then the error was back-propagated to each layer using (4). The weights are updated in order to minimise the error at the output layer. The updating formula is given in (2) and (5)

$$w_{ji}^{l,n+1} = w_{ji}^{l,n} + \Delta w_{ji}^{l,n} \tag{5}$$

where n is the iteration count. The weights are updated in each iterative step. The maximum absolute error (MAE), the average absolute error (AAE) and average root mean square error (ARMSE) are estimated by (6), (7) and (8), respectively, in each iteration

$$\text{MAE} = \max|t_i - y_i| \quad \forall i \tag{6}$$

$$\text{AAE} = \sum_{i=1}^{N_L} \left(\sum_{p=1}^{P} \frac{|t_i - y_i|}{P} \right) / N_L \tag{7}$$

$$\text{ARMSE} = \sum_{i=1}^{N_L} \left(\sum_{p=1}^{P} \frac{(t_i - y_i)^2}{P} \right) / N_L \tag{8}$$

where P is the number of input–output patterns used to train ANN. The values of MAE, AAE and ARMSE indicate accuracy of the ANN in mapping input domain to output domain.

3.2 ANN model for three-phase PVGs

The input and output variables need to be identified to build ANN model. In this case, eight inputs and six outputs are determined according to (1). The training data set can be created through measurements or simulations. A pattern of eight inputs and six outputs (targets) can be obtained in each measurement or simulation. The number and coverage of input/output domains by training data sets are very important factors in building an accurate ANN model.

In order to create training data sets through simulation, a Simulink model of PVG connecting to grid as shown in Fig. 2 is built in Matlab/Simulink software. In this Matlab/Simulink model, the temperature of photovoltaic cell Temp, the solar irradiance Irra, the three-phase PCC voltage amplitudes V_a, V_b and V_c, and phase angles φ_a, φ_b and φ_c, which are also the inputs of the proposed ANN model of PVG, can be set independently. For each simulation, the values of input variables are randomly chosen from certain ranges following uniform distribution. The range of Temp is between −20 and 35°C, and the range of Irra is between 0 and 1000 w/m^{-2}. The range of V_a, V_b and V_c is between 0.94 and 1.06 pu following uniform distribution, while the ranges of φ_a, φ_b and φ_c are −5° to 5°, −125° to −115° and 115° to 125°, respectively. The three-phase active power and reactive power flowing into the PCC, P_a, P_b, P_c, Q_a, Q_b and Q_c, which are the targets of ANN model, are recorded during simulation in the Matlab/Simulink model. The inputs and outputs of a simulation compose a training data set or set of epochs. Through simulations, 10 000 data sets are generated to train the ANN model of PVG. Min–Max data normalisation technique was used to normalise inputs and outputs for training the proposed ANN model.

Although the number of neurons in the input and output layers are determined from (1), number of hidden layers and their neurons are to be chosen. To determine the optimal configuration (number of hidden layers and neurons in each hidden layer), different configurations were trained using 1000 data sets. The criterion for termination of training is when the difference between AAEs of any two consecutive iterative steps is less than 0.00001. The AAE, MAE and convergence time of different configurations were compared and shown in Figs. 7–9. The configuration with 2 hidden layers and 14 neurons in each hidden layer has the smallest AAE as shown in Fig. 7, whereas the configuration with 2 hidden layers and 9 neurons in each hidden layer

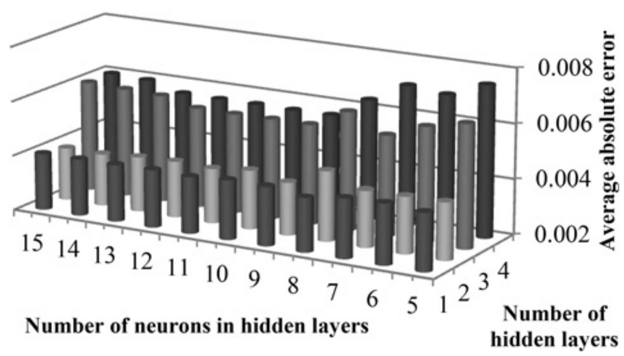

Fig. 7 *AAE of different ANN configurations*

has the smallest MAE as shown in Fig. 8. On the other hand, the training time of the former configuration is distinctly larger than the latter one (Fig. 9), but the AAE of the latter is nearly equal to the former. Hence the latter was chosen as the best configuration (two hidden layers and nine neurons in each hidden layer).

For the chosen configuration, that is, two hidden layers, nine neurons in each hidden layer, eight neurons in input layer, six neurons in output layer [corresponding to eight input and six output in (1)], the smallest ARMSE was found to be 4.985×10^{-5} when the bias of layer 1 through layer 3 were set as −2, 0 and −1.5. The configuration consists of 8 neurons in the input layer, 14 neurons in the first and the second hidden layers, and 6 neurons in the output layer. The bias values at each layer were set as −1.0, respectively. The variation of AAE along with iterations for this ANN is shown in Fig. 10.

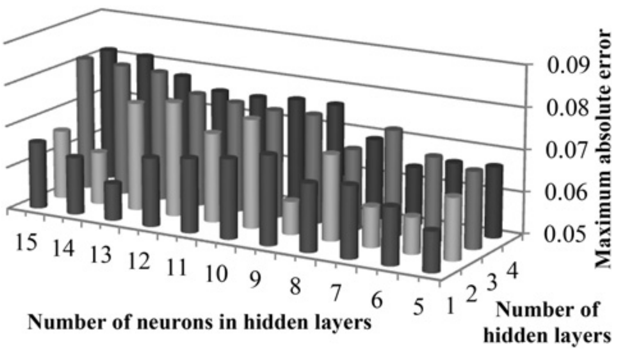

Fig. 8 *MAE of different ANN configurations*

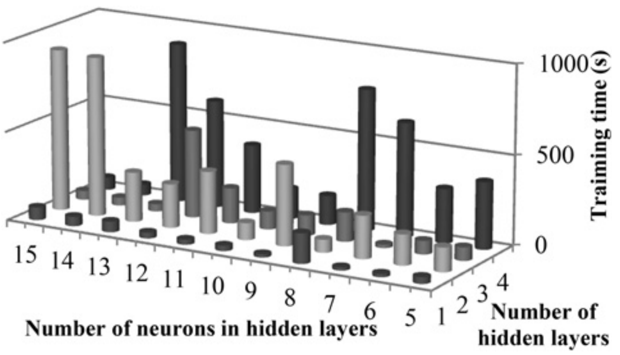

Fig. 9 *Convergence time of different ANN configurations*

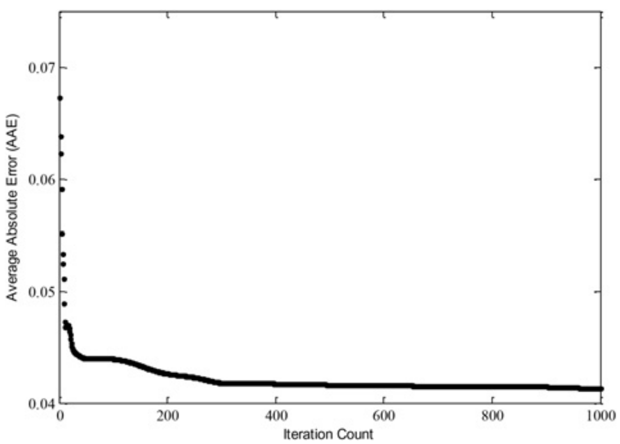

Fig. 10 *Reduction of absolute error over the number of iterations*

The graph in Fig. 10 shows reduction in the AAE with fully training for 1000 patterns within 1000 iterations. This ANN model, being a feed forward network, holds a set of matrices and it easily implementable in ladder iterative technique programs or PSS®SINCAL type commercial programs for power flow analysis.

4 Distribution system power flow study with ANN PVG model

Successful training in Section 3 shows that the proposed ANN model accurately maps the Matlab/Simulink model of PVG. In this section, the performance of the proposed ANN model of PVG is tested in power flow analysis. Although we implement the proposed ANN model in the modified ladder iterative technique, it is equally suitable for use with other methods of power flow analysis.

A 48-bus distribution system with two feeders from a Canadian utility, shown in Fig. 11, was used to assess the performance of the proposed ANN model of PVG in power flow analysis. This is an unbalanced three-phase distribution system with unbalanced loads and underground cables. The power balance equations were solved using the ladder iterative technique [7], Fig. 1. All the unbalanced network components were modelled accurately considering their mutual couplings and capacitance elements. In accurate three-phase power flow studies, PVGs have to be modeled accurately considering all the three phases. There are 21 loads in the system and 17 of them are unbalanced. The proposed ANN model of PVG was compared with fixed PQ PVG model to assess the speed and accuracy of the proposed model and solution. The ANN model of PVG that estimates power output is function of solar irradiance, temperature, and three-phase PCC voltage phasors (angle and magnitude). In the case of fixed PQ model, the power output is estimated externally using the Matlab/Simulink simulation considering the operating solar irradiance and temperature assuming rated balanced PCC voltage.

The details of power flow study include:

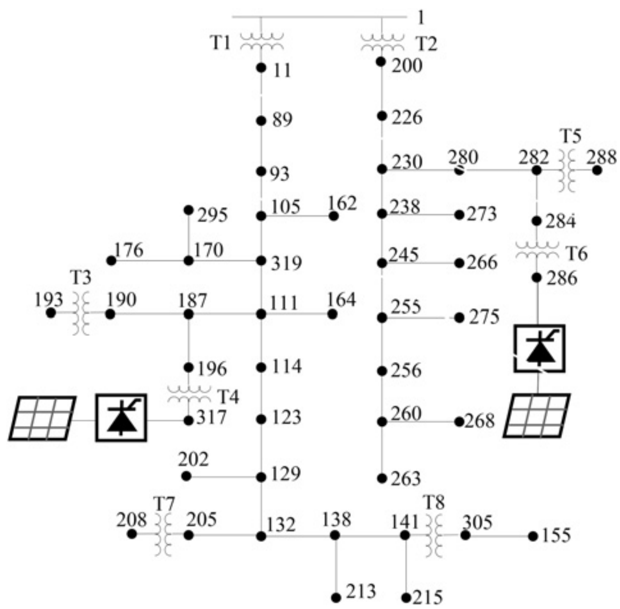

Fig. 11 *PVG connection to the distribution system (a Canadian utility)*

IET Gener. Transm. Distrib., 2014, Vol. 8, Iss. 7, pp. 1346–1353
doi: 10.1049/iet-gtd.2013.0562

(1) the transformers T1 and T2 are of 220 kV/27.6 kV 75 MVA, and other transformers are of 27.6 kV/8.32 kV 5 MVA,
(2) the rated voltage of Bus1 is 220 kV, the rated voltage of Bus193, Bus317, Bus288, Bus286, Bus208, Bus305 and Bus155 are 8.32 kV, the rated voltage of other buses is 27.6 kV,
(3) the MVA base was set to 27.6 MVA. Two power flow study cases with different PVG models were considered.

4.1 Power flow studies with two PVGs

Case 1a is a power flow study using two fixed PQ models of 1 MW connected to Bus317 and Bus286. The 1 MW fixed PQ model has negative active power loads of 328.367, 327.067 and 327.833 kW, respectively, for the three phases, and negative reactive power −0.433, 0.300 and −0.770 kVAr, respectively, for the three phases.
Case 1b is a power flow study using two fixed PQ models of 5 MW connected to Bus317 and Bus286. The 5 MW fixed PQ model has negative active power loads of 1.642, 1.635 and 1.639 MW, respectively, for the three phases, and negative reactive power 0.0022, 0.0015 and −0.0038 MVAr, respectively, for the three phases.
Case 2a is power flow study using the proposed ANN PVG model explained Section 3. This study uses two 1-MW PVGs connected to Bus317 and Bus286. The PVGs are represented using the proposed ANN model.

Except for the PVG model, all other values were the same as Case 1a. For the two power flow studies Cases 1a and 2a considering ANN and fixed PQ models, respectively, the solar irradiance and temperature were assumed equal to 900 W/m^{-2} and 25°C, respectively. For the fixed PQ model, the fixed output power corresponds 1.0 per unit balanced voltage at PCC.
Case 2b is same as case 2a except that PVGs are rated at 5 MW.

Power flow analyses were completed for cases 1a, 1b, 2a and 2b considering PVGs with ratings of 1 and 5 MW. Then voltage solutions for 1 MW PVG cases 1a and 2a were compared. This comparison is shown in Fig. 12. Similarly, voltage solutions for cases 1b and 2b considering 5 MW PVGs were compared, refer Fig. 12. These comparisons consider absolute bus voltages. Clearly, effect of larger unbalanced PVGs is more pronounced. In these studies, the ANN model of PVGs is considered more accurate as it very closely models the actual PVG as shown in Section 3.

This preceding analysis and comparisons clearly point out that the fixed PQ model, which does not consider PCC voltage, causes power flow analysis to give inaccurate solutions. Errors increase with the size of PVG.

4.2 Power flow studies with several PVGs

To further investigate errors in power flow solutions caused by using fixed PQ models of PVGs, systems with more PVGs were considered. Power flow solutions computed using fixed PQ models of PVGs were compared with power flow solutions determined using ANN model of PVGs. In addition to PVGs connected to Bus317 and Bus286, three 5 MW PVGs were connected to Bus193, Bus288 and Bus208 in steps and a power flow solutions were determined using the fixed PQ model and ANN model of PVG in each case, respectively.

The results are presented in Fig. 13. It can be found that power flow solutions computed using fixed PQ model has increasing error with additional PVGs when compared to accurate solutions computed using ANN model of PVGs. This is because the PVGs produce unbalanced power output when PCC voltage is unbalanced. PVGs in an unbalanced distribution system output unequal power in three phases further compounding the problem of unbalance.

However, as the fixed PQ model can only give the balanced output power irrespective of PCC voltage, errors in power flow solutions computed using fixed PQ model of PVGs are compounded as well.

The computational speed is a key factor in power flow algorithms. Inclusion of non-linear PVG models would significantly slowdown power flow algorithms. It must be pointed out that ANN models of PVGs are extremely efficient and suitable for fast computation. The execution times of power flow algorithm in both cases 1a and 2a with a 1 MW PVG are compared in Table 2. The proposed ANN model has a longer execution time than the fixed PQ model but has the same convergence iterations as the latter. Since PVG model computational process is just a little portion

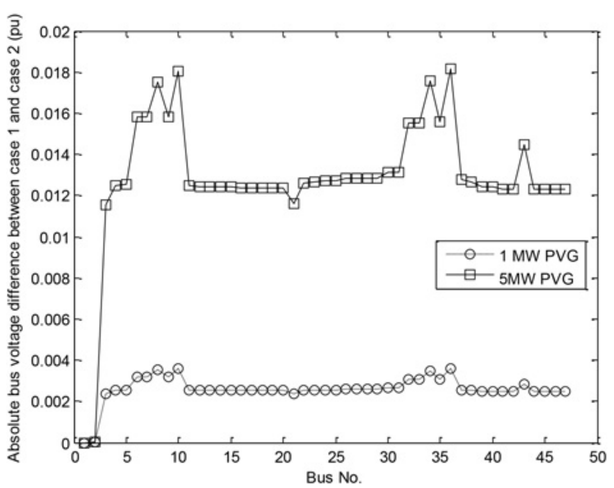

Fig. 12 *Absolute bus voltage difference between cases 1a and 2a (1 MW generators) and cases 1b and 2b (5 MW generators) are shown*

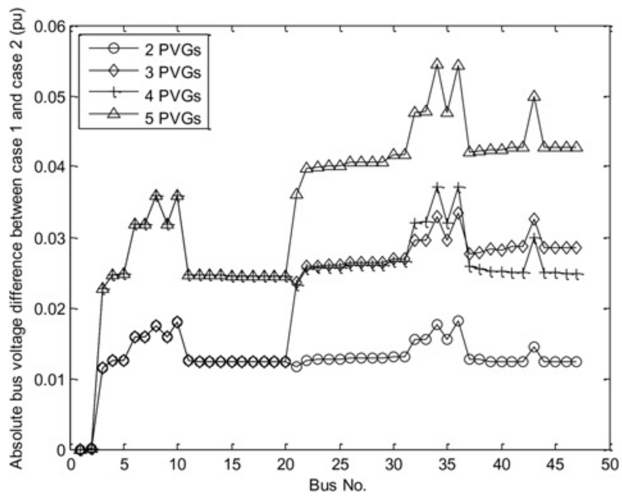

Fig. 13 *Absolute voltage difference between fixed PQ PVG model and ANN PVG model considering multiple 5 MW PVGs without additional load*

Table 2 Execution times with PVG models

	Fixed PQ	ANN
time taken for executing the model once, ms	0.005	0.508
number PF iterations	44	44
average execution time taken for the PF study, s	0.928956	0.971451

(milliseconds) of the whole power flow study program (seconds), the total execution times of two cases are quite close.

Accordingly, one may conclude that use of ANN model of PVGs does not slow the power flow analysis algorithm.

5 Implementation in commercial software packages

Another important advantage of the proposed ANN model of PVGs is that it can be integrated into commercial power system analysis software. The implementation is possible because the ANN model does not require any complex solvers or optimisation techniques to estimate the power outputs for a given set of input values. To investigate this flexibility of implementation in commercial power flow software, the ANN model of PVGs was coded in PSS®SINCAL (Siemens Network Calculator), which can solve bus-wise power balance equations of three-phase unbalanced distribution systems. At the end of each iterative step of the power flow algorithm, bus voltages are updated and then the power outputs from the PVGs are updated using ANN model.

The 48-bus distribution system shown in Fig. 11 was implemented in PSS®SINCAL (Fig. 14) with a 5 MW solar farm integrated in through Bus317 was taken as an example to show the validity of integrating ANN PVG model into PSS®SINCAL power flow analysis. PV generators are considered as negative loads and power values are updated at each power flow iterative step. In this analysis, Bus1 is connected to an external system with 107.2 MVA short-circuit power just as it is in the realistic system.

The ANN model of the PVG was coded as a Windows Script macro in PSS®SINCAL. During the solution process, the solar irradiance and temperature were fixed at 900 W/m^{-2} and 25°C, respectively. The active power output mismatch of the ANN model of PVG at the end of each iterative step of the power flow algorithm is shown in Fig. 15. When the voltage solution converges, the output of the ANN PVG model also stabilises, and the total mismatch approaches zero.

This solution from PSS®SINCAL is compared the study (case 2b) results completed in matlab script. The two solutions are identical demonstrating that the proposed ANN model of PVGs works accurately with custom developed software in matlab and the commercially used software: PSS®SINCAL. Further, it is important to point out that, on testing the proposed ANN model of PVG, it is evident that it does not cause any algorithmic stability

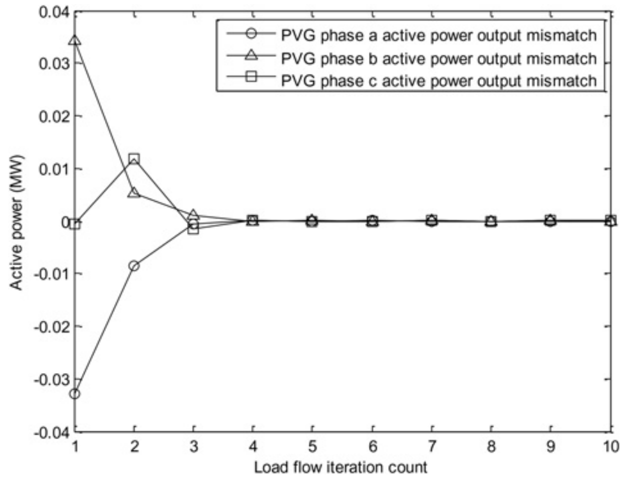

Fig. 15 *Variation of three-phase active power output mismatch of ANN PVG model in PSS®SINCAL*

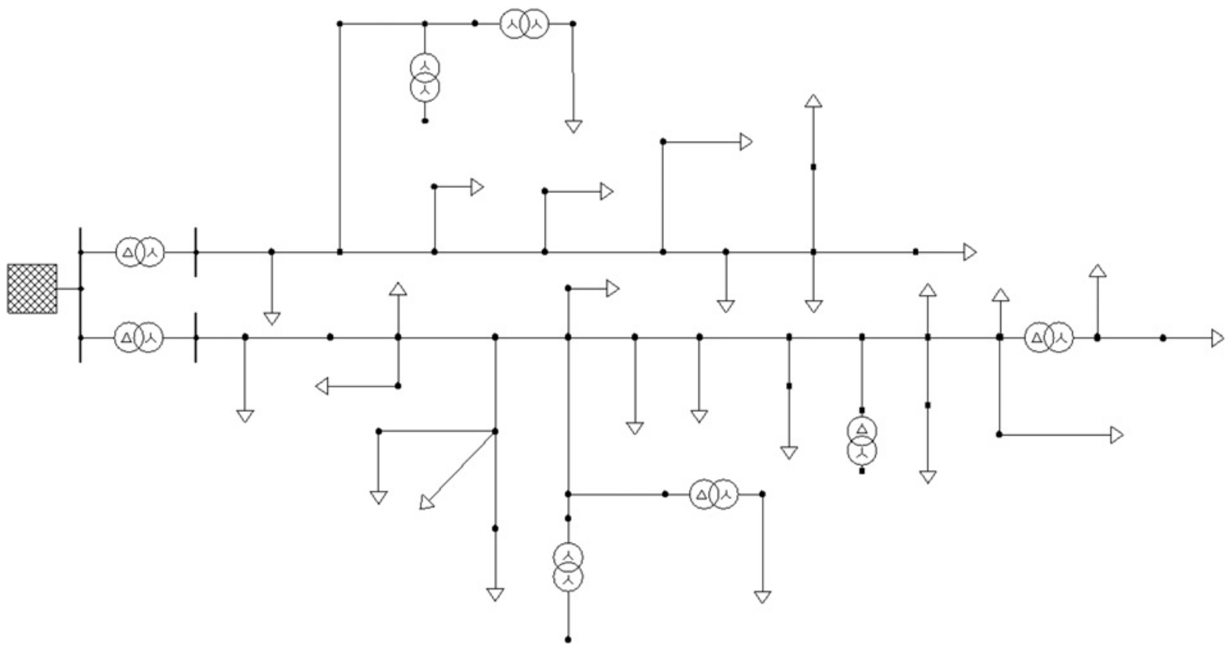

Fig. 14 *48-bus distribution system implemented in PSS®SINCAL*

doi: 10.1049/iet-gtd.2013.0562

issues with Ladder Iterative Technique or other techniques for power flow analysis used in PSS®SINCAL.

6 Conclusions

This paper presents the development of an ANN-based PVG model, tests its performance and demonstrates its ready integration into a popular commercial power system analysis software, PSS®SINCAL.

The ANN model of PVG is an accurate three-phase model which is a function of sunlight irradiance, temperature and terminal voltage phasors (magnitude and angle). It is suitable for both balanced and unbalanced three-phase systems and implementable with any type of power flow algorithm. The computational speed of ANN PVG model is almost as fast as the simplest fixed PQ model while the accuracy of the proposed model is much higher than the latter. This ANN model method is universal hence it can be trained to model any type/size of PVGs. It is readily extendable to model PVGs using measured data, and, easily extendable for modelling solar farms.

The proposed ANN model is trained using data sets from Matlab/Simulink simulations and implemented in power flow algorithms in Matlab and PSS®SINCAL. The results from this commercial software packages thus evidently prove the feasibility of applying the proposed ANN model to practical engineering power flow studies.

7 References

1 http://www.fit.powerauthority.on.ca/
2 http://www.news.ontario.ca/mei/en/2012/06/ontario-brings-more-clean-solar-power-online.html
3 Conti, S., Raiti, S.: 'Probabilistic load flow using Monte Carlo techniques for distribution networks with photovoltaic generators', *Solar Energy*, 2007, **81**, (12), pp. 1473–1481
4 Khushalani, S., Solanki, J.M., Schulz, N.N.: 'Development of three-phase unbalanced power flow using PV and PQ models for distributed generation and study of the impact of DG models', *IEEE Trans. Power Syst.*, 2007, **22**, (3), pp. 1019–1025
5 Opathella, C., Singh, B.N., Cheng, D., Venkatesh, B.: 'Intelligent wind generator models for power flow studies in PSS®E and PSS®SINCAL', *IEEE Trans. Power Syst.*, 2013, **28**, (2), pp. 1149–1159
6 Abdel-Akher, M., Nor, K.M., Rashid, AH.A.: 'Improved three-phase power-flow methods using sequence components', *IEEE Trans. Power Syst.*, 2005, **20**, (3), pp. 1389–1397
7 Kersting, W.H.: 'Distribution system modeling and analysis' (Boca Raton CRC Press, 2002)
8 Moghaddas-Tafreshi, S.M., Mashhour, E.: 'Distributed generation modeling for power flow studies and a three-phase unbalanced power flow solution for radial distribution systems considering distributed generation', *Electr. Power Syst. Res.*, 2009, **79**, (4), pp. 680–686
9 Zhu, Y., Tomsovic, K.: 'Adaptive power flow method for distribution systems with dispersed generation', *IEEE Trans. Power Deliv.*, 2002, **17**, (3), pp. 822–827
10 Thomson, M., Infield, D.G.: 'Network power-flow analysis for a high penetration of distributed generation', *IEEE Trans. Power Syst.*, 2007, **22**, (3), pp. 1157–1162
11 Salas, V., *et al.*: 'Review of the maximum power point tracking algorithms for stand-alone photovoltaic systems', *Sol. Energy Mater. Sol. Cells*, 2006, **90**, (11), pp. 1555–1578
12 Koutroulis, E., Kalaitzakis, K., Voulgaris, N.C.: 'Development of a microcontroller-based, photovoltaic maximum power point tracking control system', *IEEE Trans. Power Electron.*, 2001, **16**, (1), pp. 46–54
13 Liao, J.C., Yeh, S.N.: 'A novel instantaneous power control strategy and analytic model for integrated rectifier/inverter systems', *IEEE Trans. Power Electron.*, 2000, **15**, (6), pp. 996–1006
14 Mellit, A., Menghanem, M., Bendekhis, M.: 'Artificial neural network model for prediction solar radiation data: application for sizing stand-alone photovoltaic power system'. Proc. 2005 IEEE Power Engineering Society General Meeting, 2005, pp. 40–44
15 Mellit, A., Benghanem, M., Arab, A.H., Guessoum, A.: 'An adaptive artificial neural network model for sizing stand-alone photovoltaic systems: application for isolated sites in Algeria', *Renew. Energy*, 2005, **30**, (10), pp. 1501–1524
16 Mellit, A., Benghanem, M., Kalogirou, S.A.: 'Modeling and simulation of a stand-alone photovoltaic system using an adaptive artificial neural network: proposition for a new sizing procedure', *Renew. Energy*, 2007, **32**, (2), pp. 285–313
17 Mellit, A., Pavan, A.M.: 'Performance prediction of 20kW$_p$ grid-connected photovoltaic plant at Trieste (Italy) using artificial neural network', *Energy Convers. Manage.*, 2010, **51**, (12), pp. 2431–2441
18 Priddy, K.L., Keller, P.E.: 'Artificial neural networks an introduction'. Proc. 2005 SPIE – The Int. Society for Optical Engineering, 2005, pp. 110–116
19 Lin, W.-M., Hong, C.-M., Chen, C.-H.: 'Neural-network-based MPPT control of a stand-alone hybrid power generation system', *IEEE Trans. Power Electr.*, 2011, **26**, (12), pp. 3571–3581
20 Alam, M.J.E., Muttaqi, K.M., Sutanto, D.: 'A three-phase power flow approach for integrated 3-wire MV and 4-wire multigrounded LV networks with rooftop solar PV', *IEEE Trans. Power Electr.*, 2013, **28**, (2), pp. 1728–1737
21 Alquthami, T., Ravindra, H., Faruque, M.O., Steurer, M., Baldwin, T.: 'Study of photovoltaic integration impact on system stability using custom model of PV arrays integrated with PSS/E'. Proc. 2010 North American Power Symp. (NAPS), 2010, pp. 1–8